2000

Development of a New Electrodeposition Process for Plating of Zn-Ni-X (X = Cd, P) Alloys: Permeation Characteristics of Zn-Ni-Cd Ternary Alloys

A. Durairajan
University of South Carolina - Columbia

B. S. Haran
University of South Carolina - Columbia

Ralph E. White
University of South Carolina - Columbia, white@cec.sc.edu

Branko N. Popov
University of South Carolina - Columbia, popov@engr.sc.edu

Publication Info

Journal of the Electrochemical Society, 2000, pages 4507-4511.

Publisher's link: http://dx.doi.org/10.1149/1.1394093
DOI: 10.1149/1.1394093

Journal of The Electrochemical Society, **147** (12) 4507-4511 (2000)
S0013-4651(99)09-102-8 CCC: $7.00 © The Electrochemical Society, Inc.

Development of a New Electrodeposition Process for Plating of Zn-Ni-X (X = Cd, P) Alloys

Permeation Characteristics of Zn-Ni-Cd Ternary Alloys

A. Durairajan,* B. S. Haran, R. E. White,*** and B. N. Popov**,z**

Department of Chemical Engineering, University of South Carolina, Columbia, South Carolina 29208, USA

It is shown that an electrodeposited Zn-Ni-Cd alloy coating produced from sulfate electrolyte inhibits the discharge of hydrogen on carbon steel. The newly developed ternary alloys have approximately ten times higher corrosion resistance when compared to a Zn-Ni alloy. Hydrogen permeation characteristics of Zn-Ni-Cd alloy coatings were studied and compared with those of a bare and a Zn-Ni alloy coated steel. The transfer coefficient, α, exchange current density, i_o, thickness dependent adsorption-absorption rate constant, k'', recombination rate constant, k_3, surface hydrogen coverage, θ_H, were obtained by applying a mathematical model to experimental results. Alloys obtained from baths containing higher concentration than 3 g/L of $CdSO_4$ in the sulfate plating bath are seen to have superior permeation inhibition properties compared to the Zn-Ni alloy coating and bare steel. The hydrogen permeation current was zero under normal corroding conditions for Zn-Ni-Cd alloy and it increased to 0.3 $\mu A/cm^2$ at a cathodic overpotential of 250 mV. The hydrogen permeation current density for steel and Zn-Ni alloy under similar conditions were 62.1 and 1.3 $\mu A/cm^2$, respectively.

Manuscript submitted September 28, 1999; revised manuscript received August 31, 2000.

Hydrogen embrittlement is a serious concern that can limit the usage of various metals and alloys in different aqueous environments. Hydrogen ingress into the metal can result in the initiation of microcracks, which can later lead to the failure of the specimen.[1-3] Hydrogen embrittlement occurs as a result of hydrogen evolution on the surface of the specimen via electrochemical phenomena such as corrosion and the subsequent penetration of hydrogen into the solid following an adsorption-absorption pathway. Surface modification techniques have been used to reduce hydrogen-induced failures.[4-7] Unfortunately, processes that use heat-treatment methods and laser modification methods do not completely eliminate the hydrogen-cracking hazard while electroplating of certain materials represents promising control technique. Extensive research has been done on reducing the corrosion and hydrogen permeation of different metals in corroding environment.[8-18] Chen and Wu[8] reported the effect of copper, tin, silver, and nickel plating on hydrogen permeation inhibition in AISI 4140 steel. It was found that copper and tin effectively reduced the hydrogen permeation by over 80%. However, the corrosion resistance behavior was not presented for these electrodeposited metals. Cadmium plating has been extensively used as a corrosion resistant coating on hard steel for various applications.[9] Zamanzadeh *et al.*[10] found that deposits of cadmium reduced the hydrogen adsorption on iron. Growing ecological concerns led in recent years to attempts to exclude cadmium plating as a means of protection of steel surfaces against corrosion and hydrogen permeation.[11] Alloying of zinc with ferrous metals and in particular with nickel appeared to contain the promise of protection properties similar to those of cadmium.[12] However, an anomaly associated with the codeposition of the ferrous metals with zinc limits the barrier resistance that can be achieved with these coatings. Previously our group[13-18] has devised a variety of electrodeposition schemes to decrease corrosion and inhibit hydrogen permeation. For the hydrogen permeation inhibition, the approach has been to enhance recombination of adsorbed hydrogen atoms as hydrogen molecules as opposed to trying to control the absorption and diffusion of hydrogen into the metal.

In this study, the hydrogen permeation characteristics of Zn-Ni-Cd alloys[19] were studied under potentiostatic conditions, and the results were compared with those obtained for a Zn-Ni alloy. The corrosion studies of the Zn-Ni-Cd alloy were presented in the first part of this series.[19] Several models[20-24] have attempted to explain hydrogen entry into metals and to evaluate the kinetic and permeation parameters. In this work a potentiostatic model 23 was used for estimating the kinetic constants to enable the permeation characteristics of both alloys to be compared.

* Electrochemical Society Student Member.
** Electrochemical Society Active Member.
*** Electrochemical Society Fellow.
z E-mail: popov@engr.sc.edu

Experimental

Sample preparation.—Plating and subsequent corrosion studies were done on low-carbon steel foils with thickness of 0.5 mm and area 50 mm^2. The cleaning procedure used in this study is described by Blum *et al.*[25] Initially, the steel samples were mechanically polished with successively finer grades of emery paper, degreased with alkali, and rinsed with deionized water for 2 min. Next, the samples were treated in 20% hydrochloric acid for 1 min to remove any adherent oxide layer present on the surface and were again washed in deionized water.

Hydrogen permeation studies were carried out in the Devanathan-Stachurski[26] type permeation cell using steel foil of thickness 0.1 mm and approximately 4 cm^2 area (5 × 5 cm, Good Fellow Corporation). The same set of sample preparation procedures was adopted to insure a clean surface. One side of the membrane is carefully masked using Teflon before doing the deposition.

Electrolyte preparation and electrodeposition.—Zinc-nickel-cadmium alloys were deposited from a 0.5 M $NiSO_4$ + 0.2 M $ZnSO_4$ + 0.5 M H_3BO_3 bath in presence of $CdSO_4$ (different concentrations) and 1 g/L nonyl phenyl polyethylene oxide. Composition analysis and simple corrosion potential measurements on the resultant deposits confirmed an increase in cadmium concentration in the deposits with the increase in concentration of $CdSO_4$ in the bath until 3 g/L. The composition remained constant with further addition of $CdSO_4$.[19] Since, the composition and corrosion properties stabilized after 3 g/L $CdSO_4$ in the bath, permeation analysis was done for different concentrations of $CdSO_4$ upto 3 g/L only.

Deposition, corrosion, and permeation characterization studies were done using an EG&G PAR model 273 potentiostat interfaced with a computer. A three-electrode setup was used to deposit the alloy. The steel foils prepared as described above were used as the working electrode. Platinum foil of equal area as that of the working electrode was used as a counter electrode and a standard calomel electrode (SCE) was used as a reference electrode. All depositions were carried out potentiostatically at −1.2 V *vs.* SCE. The distance between the working and counter electrode was maintained at a constant value of 2.5 cm. The deposition time was adjusted so as to obtain a coating of thickness approximately 3 μm. All solutions

S0013-4651(99)09-102-8 CCC: $7.00

were prepared with analytical-grade reagents and distilled water. Electrochemical techniques and electrochemical impedance spectroscopy (EIS) were used to evaluate the barrier film resistance of Zn-Ni-Cd deposits. Energy dispersive spectroscopy (EDAX) was used to analyze the Zn-Ni ratio of the electrodeposits.

Since chemical dissolution of the zinc deposit occurs under acidic or alkaline conditions, the corrosion studies of Zn-Ni-Cd coatings were carried out in a 0.5 M Na_2SO_4 + 0.5 M H_3BO_3 buffer solution of pH 7.0. A three-electrode setup and an EG&G PAR model 273 potentiostat and a Solatron impedance analyzer were used to carry out the corrosion measurements. A standard calomel electrode was used as the reference and a platinum mesh electrode as the counter electrode.

Permeation experiments were carried out in a two-compartment system separated by the steel foil plated with Zn-Ni-Cd on one side. The Teflon mask on the other side is removed and the surface is carefully cleaned with soap solution followed by rinsing in distilled water. Hydrogen is evolved on the cathodic side, on the Zn-Ni-Cd deposit by potentiostatic polarization method. The electrolyte of 0.5 M Na_2SO_4 with 0.5 M H_3BO_3 buffer was used, and the pH was maintained at 7.0. The current associated with the hydrogen permeation is continuously monitored on the anodic side after setting the potential to a constant value of −0.3 V *vs.* a Hg/HgO reference electrode. The electrolyte for the anodic compartment was 0.2 M NaOH. To avoid dissolution or passivation, and to maintain consistency in the permeation current data, a thin layer of palladium was plated on the anodic side.[18] Pure nitrogen was purged through both compartments so as to keep the solutions devoid of dissolved oxygen. Permeation experiments were performed three times on new deposits to assess the reproducibility of the observed permeation currents. The observed permeation currents varied within ±3% (relative) in all cases. The average of the three readings was used for data analysis.

Results and Discussion

Addition of $CdSO_4$ to the electrolytic Zn-Ni sulfate bath lead to the codeposition of cadmium with the Zn-Ni. Zn-Ni-Cd alloys have lower corrosion potentials compared to pure Zn-Ni deposits. In Table I the corrosion potentials of deposited alloys were compared with the corrosion potentials of nickel, cadmium, and steel substrates in the corroding media (0.5 M Na_2SO_4 + 0.5 M H_3BO_3 buffer solution of pH 7.0). The observed shift in the corrosion potential from −1.13 V in case of Zn-Ni alloy to a corrosion potential of −0.635 V corresponding to Zn-Ni-Cd (3 g/L and more of $CdSO_4$ in the bath) ternary alloy coatings reflects the increase in nickel content in the alloy. The rest potential of −0.635 V *vs.* SCE for the Zn-Ni-Cd alloys is higher than the corrosion potential of Cd (−0.798 V) but lower than the corrosion potential of steel. Thus, the Zn-Ni-Cd coating offers a sacrificial protection for steel. At the same time, the overvoltage relative to the corrosion potential of steel (galvanic driving overpotential) is significantly reduced in case of Zn-Ni-Cd compared to that of Zn-Ni, thus extending the life of the coating under corroding conditions.

Electrochemical impedance spectroscopy was used to study the barrier resistance of the protective coating in corroding solutions. Figure 1 shows the Bode response of impedance analysis done on different coatings. It is seen that the low frequency resistance is about ten times higher in case of Zn-Ni-Cd (3 g/L $CdSO_4$) when compared to Zn-Ni coating. The observed increase in barrier resistance was due to an increase in the nickel content in the alloy as revealed by prior EDAX analysis[19] (6.4% Ni in the case of Zn-Ni to 20.8% Ni in the case of Zn-Ni-Cd obtained from baths containing 3 g/L $CdSO_4$). The first part of this series showed the effect of different $CdSO_4$ concentrations on the composition and corrosion properties of the deposit. Nickel and cadmium content in the alloy increased with the addition of $CdSO_4$ to the bath.[19] The results obtained from EIS and Tafel polarization studies were used to evaluate the corrosion current of the deposits in the corroding media. The polarization resistance values estimated from EIS were used to calculate the corrosion rates. Figure 2 shows a comparison of corrosion rates of various coatings. In the case of 3 g/L $CdSO_4$ (Zn-Ni-Cd alloy with Zn/Ni/Cd = 5:2:3 wt %), the corrosion rate of the resultant deposit is one order of magnitude smaller than that of the cadmium coating. This ensures the longevity of the coating for industrial applications. A much thinner coating can be used to achieve the same protection that will be obtained using a thicker cadmium coating.

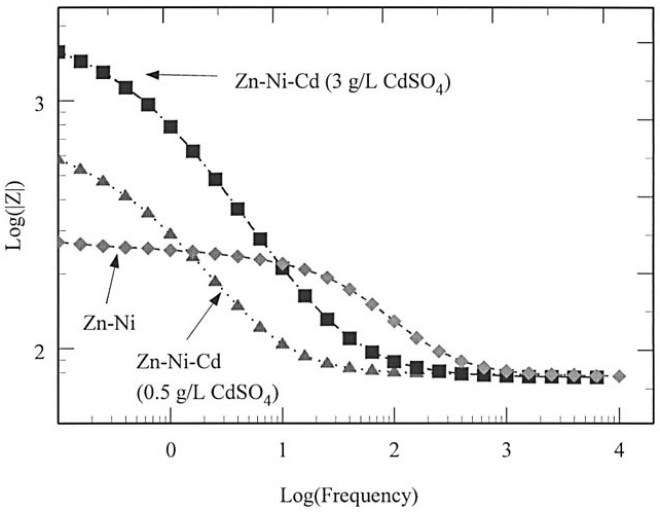

Figure 1. Bode plot of impedance response of different alloy coatings in 0.5 M H_3BO_3 + 0.5 M Na_2SO_4 (pH 7.0) solution.

Hydrogen permeation characterization.—Figure 3 shows a plot of the cathodic current density as a function of the applied overpotential for deposits obtained from baths containing different amounts of $CdSO_4$. As seen from Fig. 3, at any particular overpotential, the cathodic current density decreases (slower kinetics of hydrogen evo-

Table I. Corrosion potentials of different coatings in 0.5 M H_3BO_3 + 0.5 M Na_2SO_4 (pH 7.0) solution. (Potentials were measured with respect to a SCE electrode.)

Coating	Corrosion potential (V *vs.* SCE)
Nickel	−0.358
Cadmium	−0.780
Zn-Ni	−1.127
Zn-Ni-Cd (1 g/L $CdSO_4$)	−0.761
Zn-Ni-Cd (3 g/L $CdSO_4$)	−0.635
Steel	−0.530

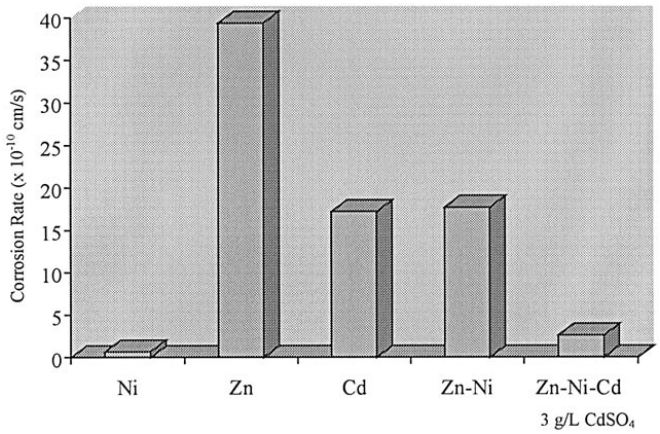

Figure 2. Comparison of corrosion rates of various alloy coatings 0.5 M H_3BO_3 + 0.5 M Na_2SO_4 (pH 7.0) solution.

S0013-4651(99)09-102-8 CCC: $7.00

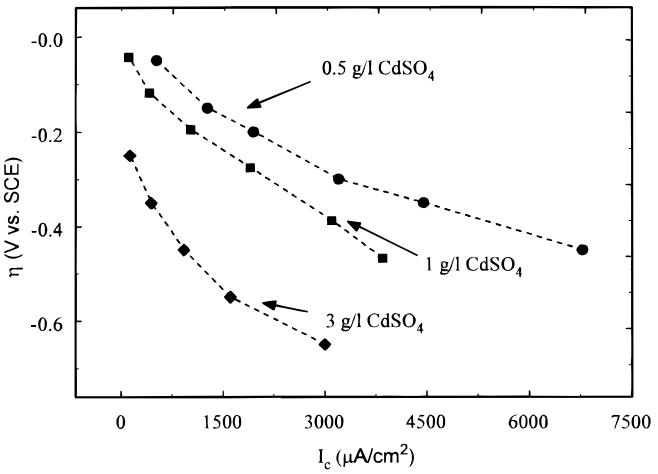

Figure 3. Plot of cathodic current densities as a function of applied overpotentials for Zn-Ni-Cd alloys containing different amounts of $CdSO_4$ in the electrolytic bath.

lution reaction) with an increase of the concentration of $CdSO_4$, which was used to deposit the coating. For a typical case of 3 g/L $CdSO_4$ in the bath, at an overpotential of −250 mV, the hydrogen evolution current density is around 10^2 μA/cm^2. At the same overpotential, for $CdSO_4$ concentration of 0.5 g/L in the bath, the deposits have a very high cathodic current density of 2000 μA/cm^2.

Figure 4 compares the permeation current densities for the deposits obtained from baths containing different amounts of $CdSO_4$ for similar range of overpotentials. A very large decrease in the permeation current density is seen for deposits obtained from sulfate electrolytes containing 3 g/L $CdSO_4$. For applied overpotentials of about −250 mV, the permeation current increased to a value of about 0.3 μA/cm^2. The increase in permeation current density was about eight times higher in case of deposits obtained from baths containing 0.5 g/L $CdSO_4$ for the same applied overpotential.

The hydrogen evolution and permeation current densities are compared in Fig. 5 for bare and Zn-Ni deposits with deposits plated from sulfate electrolytes containing 3 g/L $CdSO_4$. The cathodic and permeation current densities are about one order of magnitude smaller in case of Zn-Ni-Cd deposits when compared to Zn-Ni deposits while the hydrogen permeation current in case of steel is approximately two orders of magnitude greater than that of Zn-Ni-Cd deposits.

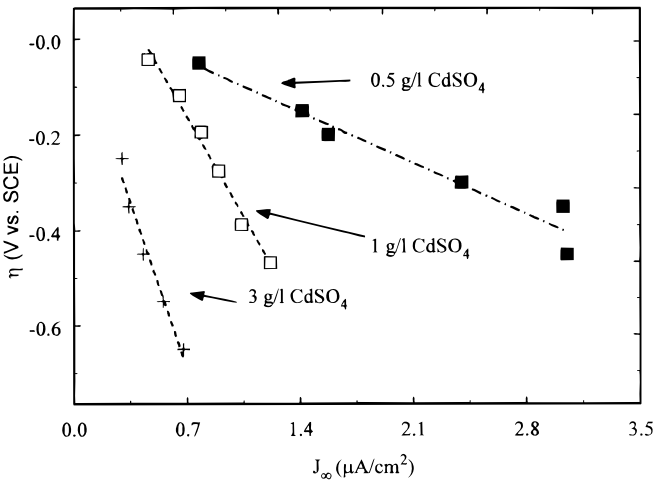

Figure 4. Plot of permeation current densities as a function of applied overpotentials for Zn-Ni-Cd alloys containing different amounts of $CdSO_4$ in the electrolytic bath.

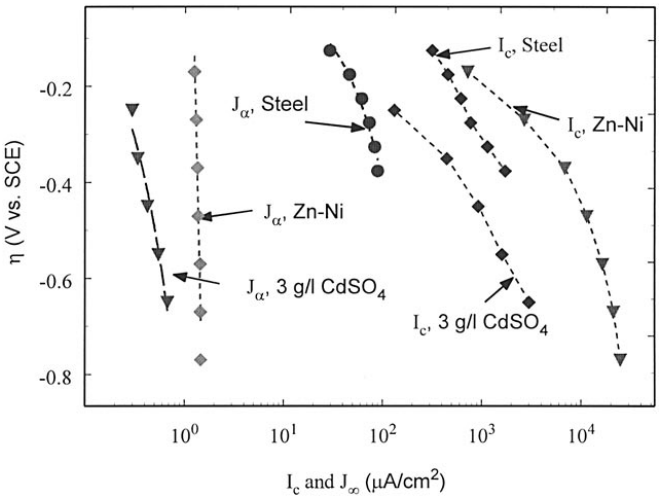

Figure 5. Comparison of cathodic and permeation current densities for Zn-Ni-Cd, Zn-Ni, and steel.

The following relationships for the permeation and cathodic current densities as a function of kinetic parameters were obtained by Iyer *et al.*[29] for the coupled discharge-chemical recombination mechanism assuming Langmuir isotherm

$$j_\infty = \frac{k''}{b\sqrt{Fk_3}}\sqrt{i_r} \qquad [1]$$

$$i_c e^{\frac{F\alpha\eta}{RT}} = -\frac{bi_0'}{k''} j_\infty + i_0' \qquad [2]$$

For this model to be applicable, the plot of j_∞ *vs.* $\sqrt{i_r}$ should be linear and pass through close to the origin. The hydrogen permeation parameters i'_0 and k'' may be evaluated from the plots j_∞ *vs.* $\sqrt{i_r}$; and $i_c e^{a\alpha\eta}$ *vs.* j_∞, respectively.

Figure 6 shows the j_∞ *vs.* $\sqrt{i_r}$ plots for Zn-Ni-Cd (3 g/L $CdSO_4$) coated and bare steel. The $i_c e^{a\alpha\eta}$ *vs.* j_∞ dependence is shown in Fig. 7. As shown in Fig. 6, in the case of Zn-Ni-Cd alloy coating, deviations occur in the square root relationship. This nonlinearity arises due to the activation of hydrogen evolution reaction.[28] Under these conditions, the Frumkin-Temkin (F-T) corrections have to be applied to the discharge and recombination currents.[28] Equations 3 and 4 give the modified set of charging and recombination currents[29]

$$i_c = i_0'(1 - \theta_H)e^{-\frac{F\alpha\eta}{RT}} e^{-\alpha f'\theta_H} \qquad [3]$$

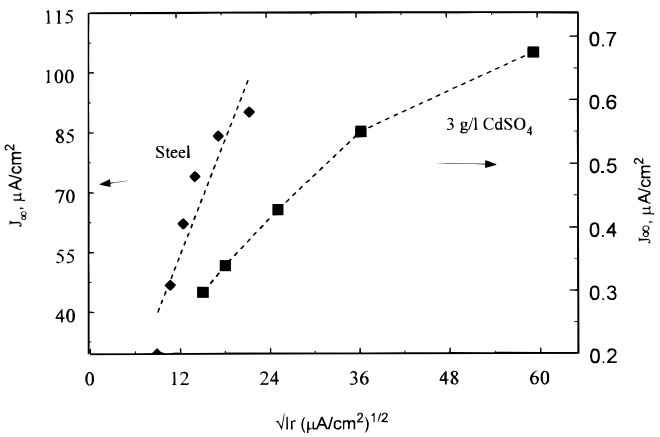

Figure 6. Plots of the hydrogen permeation current *vs.* square root of the recombination current for Zn-Ni-Cd (3 g/L $CdSO_4$) and steel.

S0013-4651(99)09-102-8 CCC: $7.00

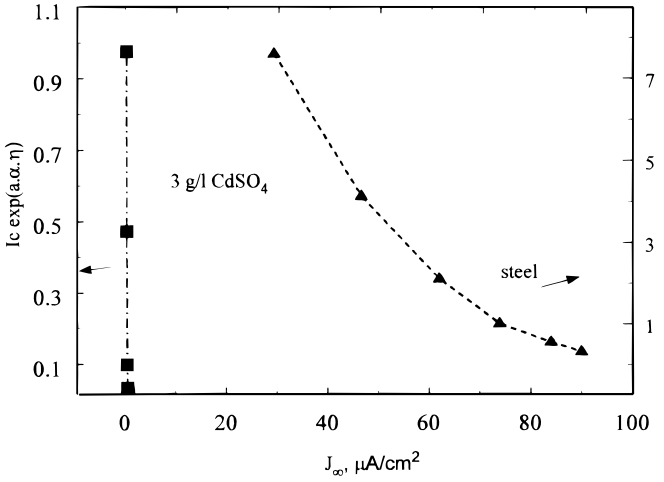

Figure 7. Plots of the hydrogen charging function ($I_c e^{a\alpha\eta}$) *vs*. steady-state hydrogen permeation current (j_∞) for Zn-Ni-Cd (3 g/L $CdSO_4$) and steel.

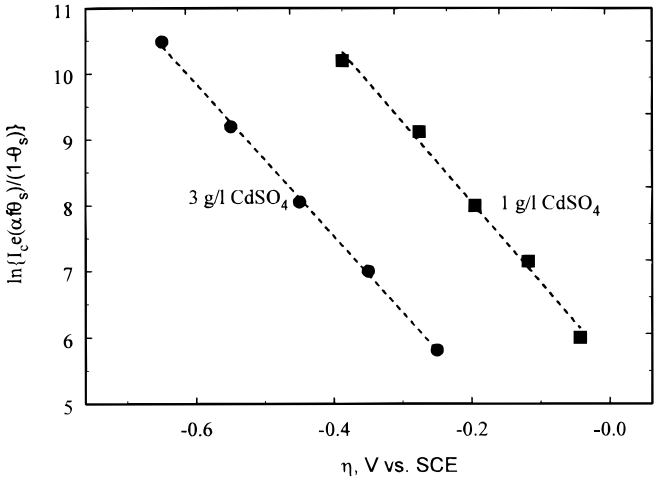

Figure 9. Plot of hydrogen coverage corrected i_c *vs*. hydrogen overvoltage, η, for different Zn-Ni-Cd deposits.

$$i_r = Fk_3\theta_H^2 e^{2\alpha f'\theta_H} \quad [4]$$

where $f' = \gamma/RT$ and γ is the gradient of the apparent standard free energy of adsorption with coverage. The value of f' is taken to be equal to 4.5.[28] After suitable modifications, Eq. 3 and 4 can be written as

$$\ln\{i_c e^{(\alpha f' b j_\infty/k'')}/(1 - bj_\infty/k'')\} = -\alpha a\eta + \ln(i_o') \quad [5]$$

$$\ln(\sqrt{i_r}/j_\infty) = (\alpha f' b/k'')j_\infty + \ln\{b(Fk_3)^{0.5}/k''\} \quad [6]$$

The nonlinear trend in the j_∞ *vs*. $\sqrt{i_r}$ arises as a result of the exponent term added to the characterizing currents to compensate for the higher surface coverage.

As shown in Fig. 8, a plot of ln ($\sqrt{i_r}/j_\infty$) *vs*. j_∞ shown for Zn-Ni-Cd coatings deposited from 1 and 3 g/L $CdSO_4$ is linear. The parameters of interest were evaluated using the slopes and intercepts of plotting functions 11 and 12 (Fig. 8 and 9) by an iterative procedure. The value of α was assumed to be 0.5 for the first guess. With this value for α, the constant k'' can be obtained from the slope of plot ln ($\sqrt{i_r}/j_\infty$) *vs*. j_∞ (Fig. 8). The recombination rate constant k_3 can be determined from the intercept of the same plot.

The exchange current density i_o is determined from the $\ln\{i_c e^{(af'\theta_H)}/(1-\theta_H)\}$ *vs*. η plot (Fig. 9). Knowing the i_o from the intercept of the plot, we proceed to verify the α value assumed. Using this α value obtained from the regression analysis of Eq. 11, a new value for k'' was found by a regression analysis of Eq. 6. Next, a regression analysis is again performed on Eq. 5. The procedure was repeated until α converges to a fixed value. Having calculated k'', θ_H can be calculated using the relation

$$\theta_H = b\frac{j_\infty}{k''} \quad [7]$$

Figure 10 shows the hydrogen surface coverage (θ_H) as a function of the overpotential. The surface coverage is quite high in case of Zn-Ni-Cd alloys. However, the enhancement on the recombination, which is shown later, ensures lesser hydrogen permeation. Data analysis has been done previously for Zn-Ni case and plain steel.[24] The results are presented along with our findings for Zn-Ni-Cd alloys for the sake of comparison.

Table II summarizes the different constants that characterize the hydrogen permeation in Zn-Ni-Cd alloy obtained from baths containing 1 and 3 g/L of $CdSO_4$. Constants evaluated for Zn-Ni are also shown for comparison. A diffusion coefficient[24] value of 2.67×10^{-7} cm^2/s was used for these analyses. The thickness of the coating was assumed to be negligible when compared to the thickness of the steel membrane, and hence any effect of the coating on the diffusion of hydrogen is neglected. The accuracy of the computed values of transport and kinetic properties are primarily dependent on the accuracy of the diffusivity value. It is seen from the table that the

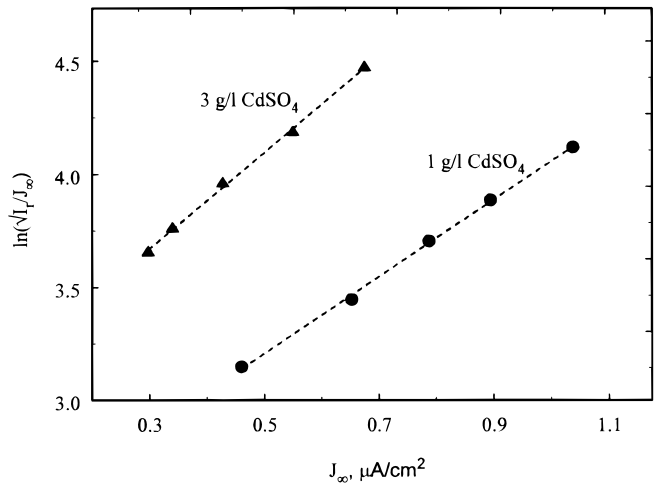

Figure 8. Relationship between $\ln(i_r^{0.5}/j_\infty)$ and j_∞ for different Zn-Ni-Cd deposits.

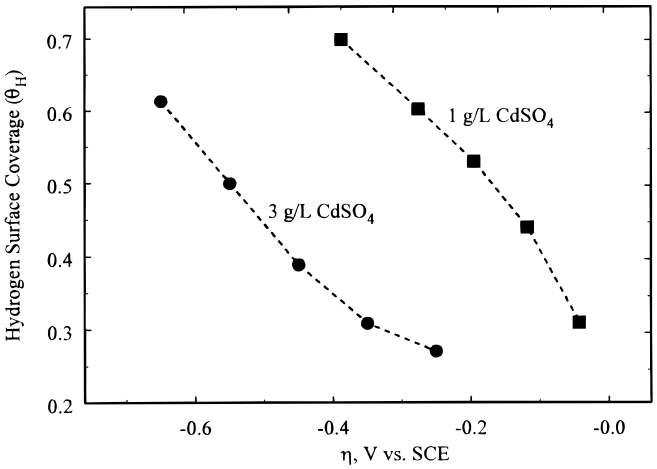

Figure 10. Plot of surface hydrogen coverage, θ_H, *vs*. hydrogen overvoltage, η, for different Zn-Ni-Cd deposits.

S0013-4651(99)09-102-8 CCC: $7.00

Table II. The different kinetic parameters characterizing the hydrogen ingress through various alloys.

	Steel	Zn-Ni	Zn-Ni-Cd (1 g/L $CdSO_4$)	Zn-Ni-Cd (3 g/L $CdSO_4$)
i_o, A/cm^2	6.98×10^{-4}	5.66×10^{-4}	2.61×10^{-4}	2.05×10^{-5}
k'', mol/cm^3	2.85×10^{-9}	4.05×10^{-9}	5.92×10^{-7}	4.39×10^{-7}
k_3, mol/cm^2 s	1.58×10^{-15}	3.9×10^{-12}	1.78×10^{-10}	2.54×10^{-10}

i_o value for Zn-Ni largely decreases with the addition of $CdSO_4$ in the electrolytic bath. This decrease reflects the slower kinetics of hydrogen evolution on deposits obtained from baths containing $CdSO_4$. The surface coverage of hydrogen decreases with the addition of $CdSO_4$ in the bath (Fig. 10). However, there is a tremendous increase in the value of recombination rate constant, k_3, suggesting higher recombination rate in case of Zn-Ni-Cd alloys when compared to Zn-Ni. It is interesting to note that the adsorption-absorption coefficient increases in case of Zn-Ni-Cd alloys. This increase however, does not greatly affect the hydrogen permeation in the alloy because most of the hydrogen present on the surface is recombined. Thus, the increase in recombination rate constant counters the effect due to the increased adsorption-absorption rate constant. This ensures a decrease of hydrogen permeation through the membrane. Hence concentration of 3 g/L (and above) of $CdSO_4$ in the bath would lead to deposits with inhibition toward hydrogen permeation.

Conclusions

Impedance analysis on Zn-Ni-Cd alloys indicated better barrier resistance when compared to Zn-Ni alloys. The hydrogen permeation characteristics of these coatings on steel were evaluated under cathodically polarized conditions and were compared with the Zn-Ni coated steel and plain steel. Frumkin-Tempkin isotherm was adopted in order to account for the effects of a large surface coverage of hydrogen. The modified Iyer, Pickering, and Zamanzadeh model was used to determine the transport and kinetics parameters of these deposits. It is seen that the exchange current density decreases with increasing concentration of $CdSO_4$ in the bath. Also the recombination rate constant increases with the addition of $CdSO_4$ to the electrolytic bath. This ensures a decrease of the amount of hydrogen available for absorption. An increase in the adsorption-absorption rate constant was observed. The observed decrease in hydrogen permeation rate through Zn-Ni-Cd (3 g/L $CdSO_4$) was due to both the decrease in the corrosion current density and an increase in the recombination rate constant.

Acknowledgments

Financial support by A. John Sedriks, the Office of Naval Research, under contract no. N00014-98-10053, is gratefully acknowledged.

The University of South Carolina assisted in meeting the publication costs of this article.

List of symbols

a	a constant, F/RT, V^{-1}
A	amperes
b	a constant, L/FD, mol (A cm)$^{-1}$
D	hydrogen diffusion coefficient, cm^2 s^{-1}
F	Faradayís constant, 96,487 C/equiv^{-1}
f'	a constant = γ/RT, dimensionless
i_c	charging current density, A cm^{-2}
j_∞	steady-state permeation flux, A cm^{-2}
i_r	steady-state recombination flux, A cm^{-2}
i_o	exchange current density, A cm^{-2}
k_1	discharge reaction rate coefficient, mol (cm^2 s)$^{-1}$
k_3	recombination rate constant, mol (cm^2 s)$^{-1}$
k_{abs}	absorption rate constant, mol (cm^2 s)$^{-1}$
k_{ads}	adsorption rate constant, cm s^{-1}
k''	thickness dependent absorption-adsorption rate constant, mol cm^{-3}
L	membrane thickness, cm
R	gas constant, 8.314 J (g mol k)$^{-1}$
T	temperature, K

Greek

α	transfer coefficient, dimensionless
η	overvoltage, V
θ_H	surface hydrogen coverage, dimensionless
γ	gradient of the apparent standard free energy of adsorption with hydrogen coverage, J g mol^{-1}

References

1. P. Subramanyan, in *Comprehensive Treatise of Electrochemistry*, Vol. 4, J. O.'M. Bockris, B. E. Conway, E. A. Yeager, and R. E. White, Editors, p. 411, Plenum Press, New York (1981).
2. C. L. Ho and S. L. I. Chan, in *Proceedings of 3rd Asian Coating Forum*, p. 243, Taipei, Taiwan (1990).
3. D. B. McDonnell, V. S. Sastri, C. Tian, and J. Bednar, *Metall Trans. A*, **16**, 1694 (1985).
4. A. J. Kumnick and H. H. Johnson, *Metall. Trans. A*, **6**, 1,087 (1975).
5. B. E. Wilde and T. Shimida, *Scr. Metall.*, **22**, 551 (1988).
6. R. H. Song and S. Pyun, *J. Electrochem. Soc.*, **137**, 1051 (1990).
7. C. Mergey, *Br. Corros. J.*, **19**, 132 (1984).
8. J. M. Chen and J. K. Wu, *Plat. Surf. Finish*, **33**, 657 (1992).
9. K. R. Baldwin and C. J. E. Smith, *Trans. Inst. Met. Finish.*, **74**, 202 (1996).
10. M. Zamanzadeh, A. Allam, C. Kato, B. Ateya, and H. W. Pickering, *J. Electrochem. Soc.*, **129**, 284 (1982).
11. D. McLandolt, *Electrochim. Acta*, **39**, 1075 (1994).
12. J. W. Dini and H. R. Johnson, *Met. Finish.*, **77**, 31 (1979).
13. B. N. Popov, G. Zheng, and R. E. White, *Corrosion*, **50**, 613 (1994).
14. B. N. Popov, G. Zheng, and R. E. White, *Corrosion*, **51**, 429 (1995).
15. G. Zheng, B. N. Popov, and R. E. White, *J. Elecrochem. Soc.*, **140**, 3,153 (1993).
16. G. Zheng, B. N. Popov, and R. E. White, *J. Elecrochem. Soc.*, **141**, 1,220 (1994).
17. G. Zheng, B. N. Popov, and R. E. White, *J. Elecrochem. Soc.*, **141**, 1,526 (1994).
18. B. N. Popov, G. Zheng, and R. E. White, *Corros. Sci.*, **36**, 2,139 (1994).
19. A. Durairajan, B. S. Haran, B. N. Popov, and R. E. White, *J. Electrochem. Soc.*, **147**, 48 (2000).
20. J. McBreen, L. Nanis, and W. Beck, *J. Electrochem. Soc.*, **113**, 1218 (1966).
21. B. S. Chaudhari and T. P. Radhakrishnan, *Surf. Technol.*, **22**, 353 (1984).
22. S. K. Yen and H. C. Shih, *J. Electrochem. Soc.*, **135**, 1169 (1988).
23. R. N. Iyer, H. W. Pickering, and M. Zamanzadeh, *J. Electrochem. Soc.*, **136**, 2,463 (1989).
24. M. Ramasubramanian B. N. Popov, and R. E. White, *J. Electrochem. Soc.*, **145**, 1907 (1998).
25. W. Blum and G. B. Hogaboom, *Principles of Electroplating and Electroforming*, 3rd ed., p. 200, McGraw Hill Book Co. Inc., New York (1949).
26. M. A. V. Devanathan and Z. Stachurski, *Proc. Roy. Soc. London, Series A*, **270**, 90 (1962).
27. A. Durairajan, B. N. Popov, M. Ramani, A. Krishniyer, B. S. Haran, and R. E. White, Abstract 94, The Electrochemical Society Meeting Abstracts, Vol. 99-1, Seattle, WA, May 2-6, 1999.
28. E. Gileadi and B. E. Conway, in *Modern Aspects of Electrochemistry*, J. O. M. Bockris and B. E. Conway, Editors, No. 3, pp. 347-442, Butterworths, Washington, DC (1964).
29. R. N. Iyer, I. Takeuchi, M. Zamanzadeh, and H. W. Pickering, *Corrosion*, **46**, 480 (1990).